The 2010 IEEE/RSJ International Conference on
Intelligent Robots and Systems
October 18-22, 2010, Taipei, Taiwan

Modeling and Property Estimation of Japanese Sweets for Their Manufacturing Simulation

Zhongkui Wang and Shinichi Hirai

Abstract— **Traditional Japanese sweets have long history and intense cultural background. In order to automate the manufacture process and also hand down the skillful techniques of sweets making, it is necessary to investigate the mathematical models of such objects and estimate their physical properties. This paper introduced a five-element physical model to describe the deformation behaviors of such materials. Using finite element (FE) method, a 2D/3D FE dynamic model was formulated to simulate arbitrary shaped objects. An approach for estimating physical parameters was then proposed based on FE simulation and nonlinear optimization. To capture both forces and deformation behaviors, two sets of parameters were identified and employed to simulate real Japanese sweets. A series of experimental results validated the FE model and property estimation method.**

I. INTRODUCTION

The modeling of soft objects, including human organs and tissues, cloth, and various food products, has been studied more than 20 years [1], [2]. Many applications have been involved, such as surgical simulation [3], robot grasping [4], and food engineering [5]. Comparing with elastic or viscoelastic objects such as rubber and most living organs, food materials demonstrate more complicated behaviors. It often yields residual deformation when such materials are subjected to operations, such as pushing or pulling. It is difficult to model the residual deformation. However in our living life, there are many kinds of food materials, such as sweets, which exhibit this deformation behavior. Particularly in Japan, there are many kinds of delicate and elegant sweets due to the traditional sweets culture. In resent years, the sweets market in Japan has been enlarged because of the prosperity of tea ceremony and the increase of health oriented movements [6]. Therefore, automatic manufacture systems have started to be introduced into Japanese sweets industries and the number of sweets made by machines is increasing. On the other hand, making such delicate sweets required some skillful techniques and an novice has to be trained for long time to master these techniques [6]. In order to simulate the manufacturing process and hand down these skillful techniques, it is necessary to model such sweets materials and estimate their physical properties.

For modeling soft deformable objects, several modeling methods have been used frequently, such as: mass-spring-damper (MSD) method [7], the finite difference method (FDM) [1], the boundary element method (BEM) [8], and the finite element method (FEM) [9]. The simulation accuracy and computation cost also increased in this order. Along with the development of computer technology, FEM became the most popular method for modeling deformable objects. However, most researches have focused on elastic or viscoelastic deformation, whose deformation was able to recover completely after arbitrary operations. There are very few researches dealing with sweets-like objects. MSD method has been employed to model a food dough and the physical parameters were then calibrated using GA optimization [10], [11]. MSD method has one advantage of less computation costs, but simulation accuracy is quite limited. A sushi was modeled by a two-layered Maxwell model for simulating the grasping motion [12] and the physical properties were calculated based on curve fitting [13]. In addition, the ISU exoskeleton technique has been used to model a clay and simulate the interaction between virtual clay and a human finger [14]. However, none of them employed FEM to model their targets.

In our previous works, we first developed a MSD model for simulating food products utilizing three-element [15] and four-element [16] physical models, respectively. Based on this model, we proposed an approach to extract the material properties through a "touch and see" experiment [17]. To improve the simulation accuracy, FE models has been developed for simulating three types of deformable objects: elastic, visco-plastic, and rheological objects [18]. Based on the FE model, we attempted to calculate the physical parameters by fitting the experimental force curve to a least squares plot [19]. We found that three-element physical model could only capture the deformed shape during pushing or keeping operations, while the force approximation experienced big errors. We then employed the four-element model to describe these behaviors and utilized an optimization process to estimate the physical parameters [20]. It turned out that we could approximate the force behavior pretty well but the final-shape (stable shape after releasing) again experienced big error.

In this paper, we introduced five-element physical model associated with FEM to model sweets-like objects. Using nonlinear optimization algorithm, we estimated two sets of physical parameters for capturing both deformed shapes and force behaviors, respectively. During simulation, both sets of parameters were input into the simulator but only corresponding desired results were output to the user. Experimental results with typical materials of Japanese sweets were then presented to validate our FE model and parameter estimation method.

The authors are with the Department of Robotics, Ritsumeikan University, Noji-Higashi 1-1-1, Kusatsu, Shiga 525-8577 Japan. gr046074@ed.ritsumei.ac.jp, hirai@se.ritsumei.ac.jp.

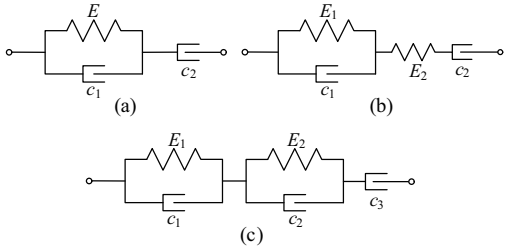

Fig. 1. The physical models for describing behaviors of rheological objects: (a) The three-element, (b) the four-element, and (c) the five-element models.

The remainder of this paper is organized as follows: FE dynamic model is presented in Section 2. Section 3 discusses the method for estimating physical properties. Experiment and validation results are given in Section 4, followed by a conclusion and discussion of future work in Section 5.

II. FE DYNAMIC MODEL

A. Introduction of Physical Models

Two popular physical models have been used to describe the behaviors of rheological (sweets-like) objects. They are the three-element and the four-element physical models, as shown in Fig. 1a and 1b. Based on our knowledge, the three-element model can not accurately capture force behaviors of rheological deformation because there is only one exponential function in the force expression of this model. The four-element model can reach a good force approximation, but vibration in force results existed because of an independent elastic element (denoted by E_2) connected in series (Fig. 1b). We therefore introduce five-element physical model (Fig. 1c) in this paper. By using this model, we were able to obtain more accurate results.

A five-element physical model consists of two elastic elements, E_1, and E_2, and three viscous elements, c_1, c_2, and c_3 (Fig. 1c). An elastic element connected to a viscous element in parallel is called a Voigt element. In other words, a five-element model consists of two Voigt elements and a viscous element connected in serial. Let ε_1^{voigt}, ε_2^{voigt}, and ε^{vis} be strains at the left Voigt, middle Voigt, and right viscous elements, respectively. Let ε be strain at the five-element model and σ be stress applied to the model. The strain ε therefore equal to the sum of the strains at all the left, middle Voigt and right viscous elements. The stress σ is equal to the stress caused by each element. That is,

$$\begin{aligned}&\varepsilon = \varepsilon_1^{voigt} + \varepsilon_2^{voigt} + \varepsilon^{vis},\\ &\sigma = E_1\varepsilon_1^{voigt} + c_1\dot{\varepsilon}_1^{voigt} = E_2\varepsilon_2^{voigt} + c_2\dot{\varepsilon}_2^{voigt} = c_3\dot{\varepsilon}^{vis}.\end{aligned} \tag{1}$$

From the above equations, we have the following differential equation that illustrates the constitutive law of stress and strain for the five-element physical model.

$$\ddot{\sigma} + A_1\dot{\sigma} + A_0\sigma = B_2\dddot{\varepsilon} + B_1\ddot{\varepsilon} + B_0\dot{\varepsilon}, \tag{2}$$

where A_0, A_1, B_0, B_1, and B_2 are five coefficients which can be calculated by five physical parameters E_1, E_2, c_1, c_2 and c_3 as follows:

$$\begin{aligned}A_0 &= \frac{E_1E_2}{c_1c_2 + c_2c_3 + c_3c_1}, \quad A_1 = \frac{E_1(c_2+c_3) + E_2(c_1+c_3)}{c_1c_2 + c_2c_3 + c_3c_1},\\ B_0 &= \frac{E_1E_2c_3}{c_1c_2 + c_2c_3 + c_3c_1}, \quad B_1 = \frac{E_1c_2c_3 + c_1E_2c_3}{c_1c_2 + c_2c_3 + c_3c_1},\\ B_2 &= \frac{c_1c_2c_3}{c_1c_2 + c_2c_3 + c_3c_1}.\end{aligned} \tag{3}$$

B. FE Dynamic Model

In FE modeling, an object is described by a set of triangles (2D case) or tetrahedra (3D case). Dynamic behaviors of the object are then formulated by the behaviors of individual triangles or tetrahedra. In this paper, we formulate 2D deformation of a rheological object with thickness of h. The object is constructed by a set of triangles and a five-element physical model is imposed on each triangle to govern the strain-stress relationship, as shown in Fig. 2. Follow the same derivation process as [20], the force vector generated on all nodal points can be expressed as:

$$\mathbf{F}_{2D}^{rheo} = \mathbf{J}_\lambda(\omega_1^\lambda - \omega_2^\lambda) + \mathbf{J}_\mu(\omega_1^\mu - \omega_2^\mu), \tag{4}$$

where

$$\begin{aligned}\omega_1^\lambda &= \frac{1}{m-n}\int_0^t e^{-n(t-t')}[B_0^\lambda\dot{\mathbf{u}}_N(t') + (B_1^\lambda - nB_2^\lambda)\ddot{\mathbf{u}}_N(t')]\,\mathrm{d}t',\\ \omega_1^\mu &= \frac{1}{m-n}\int_0^t e^{-n(t-t')}[B_0^\mu\dot{\mathbf{u}}_N(t') + (B_1^\mu - nB_2^\mu)\ddot{\mathbf{u}}_N(t')]\,\mathrm{d}t',\\ \omega_2^\lambda &= \frac{1}{m-n}\int_0^t e^{-m(t-t')}[B_0^\lambda\dot{\mathbf{u}}_N(t') + (B_1^\lambda - mB_2^\lambda)\ddot{\mathbf{u}}_N(t')]\,\mathrm{d}t',\\ \omega_2^\mu &= \frac{1}{m-n}\int_0^t e^{-m(t-t')}[B_0^\mu\dot{\mathbf{u}}_N(t') + (B_1^\mu - mB_2^\mu)\ddot{\mathbf{u}}_N(t')]\,\mathrm{d}t'.\end{aligned} \tag{5}$$

Definition for matrix $\mathbf{J}_\lambda$, $\mathbf{J}_\mu$, and variables m, n, B_0^λ, B_1^λ, B_2^λ, B_0^μ, B_1^μ and B_2^μ can be found in [20].

Supposing that an object was fixed on the ground and the top surface of the object was pushing down with a displacement function of $d(t)$. These two constraints can be formulated as follows by using constraint stabilization method (CSM) [21].

$$\begin{aligned}\mathbf{A}^T\ddot{\mathbf{u}}_N + \mathbf{A}^T(2\psi\dot{\mathbf{u}} + \psi^2\mathbf{u}_N) = 0.\\ \mathbf{B}^T(\ddot{\mathbf{u}}_N - \ddot{\mathbf{d}}) + \mathbf{B}^T[2\psi(\dot{\mathbf{u}}_N - \dot{\mathbf{d}}) + \psi^2(\mathbf{u}_N - \mathbf{d})] = 0.\end{aligned} \tag{6}$$

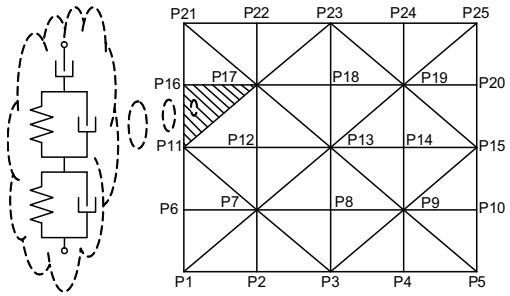

Fig. 2. 2D FE model with five-element model imposed on each triangle.

where matrix $\mathbf{A}$ and $\mathbf{B}$ denotes which nodal points should be constrained on the bottom and top surface, respectively. Scalar ψ was a predetermined angular frequency and was set to 2000 for both constraints.

Let $\mathbf{M}$ be an inertia matrix and $\boldsymbol{\lambda_1}$ and $\boldsymbol{\lambda_2}$ be the Lagrange multipliers which denote a set of constraint forces corresponding to both geometric constraints. Using the Lagrange dynamic method, a set of dynamic equations of the nodal points are given by

$$-\mathbf{J}_\lambda(\omega_1^\lambda-\omega_2^\lambda)-\mathbf{J}_\mu(\omega_1^\mu-\omega_2^\mu)+\mathbf{A}\boldsymbol{\lambda_1}+\mathbf{B}\boldsymbol{\lambda_2}-\mathbf{M}\ddot{\mathbf{u}}_N=0. \tag{7}$$

Consequently, by introducing velocity vector $\mathbf{v}_N=\dot{\mathbf{u}}_N$, a set of dynamic equations for FE simulation can be described as:

$$\begin{aligned}
\dot{\mathbf{u}}_N &= \mathbf{v}_N,\\
\mathbf{M}\dot{\mathbf{v}}_N-\mathbf{A}\boldsymbol{\lambda_1}-\mathbf{B}\boldsymbol{\lambda_2} &= -\mathbf{J}_\lambda(\omega_1^\lambda-\omega_2^\lambda)-\mathbf{J}_\mu(\omega_1^\mu-\omega_2^\mu),\\
-\mathbf{A}^T\dot{\mathbf{v}}_N &= \mathbf{A}^T(2\psi\mathbf{v}_N+\psi^2\mathbf{u}_N),\\
-\mathbf{B}^T\dot{\mathbf{v}}_N &= \mathbf{B}^T[2\psi(\mathbf{v}_N-\dot{\mathbf{d}})+\psi^2(\mathbf{u}_N-\mathbf{d})]-\mathbf{B}^T\ddot{\mathbf{d}},\\
-\frac{B_1^\lambda-nB_2^\lambda}{m-n}\dot{\mathbf{v}}_N+\dot{\omega}_1^\lambda &= -n\omega_1^\lambda+\frac{B_0^\lambda}{m-n}\mathbf{v}_N,\\
-\frac{B_1^\mu-nB_2^\mu}{m-n}\dot{\mathbf{v}}_N+\dot{\omega}_1^\mu &= -n\omega_1^\mu+\frac{B_0^\mu}{m-n}\mathbf{v}_N,\\
-\frac{B_1^\lambda-mB_2^\lambda}{m-n}\dot{\mathbf{v}}_N+\dot{\omega}_2^\lambda &= -m\omega_2^\lambda+\frac{B_0^\lambda}{m-n}\mathbf{v}_N,\\
-\frac{B_1^\mu-mB_2^\mu}{m-n}\dot{\mathbf{v}}_N+\dot{\omega}_2^\mu &= -m\omega_2^\mu+\frac{B_0^\mu}{m-n}\mathbf{v}_N,
\end{aligned} \tag{8}$$

where the last four equations were obtained by differentiating (5) with respect to time t. Note that the above linear equations are solvable since the coefficient matrix is regular, implying that we can compute $\dot{\mathbf{u}}_N$, $\dot{\mathbf{v}}_N$, $\dot{\omega}_1^\lambda$, $\dot{\omega}_1^\mu$, $\dot{\omega}_2^\lambda$, and $\dot{\omega}_2^\mu$. Thus, we can obtain the integrals of these variables using the Runge-Kutta method and finally compute the displacements and forces. Detailed information about how to calculate matrices $\mathbf{J}_\lambda$, $\mathbf{J}_\mu$, $\mathbf{M}$ and how to impose geometric constraints (matrix $\mathbf{A}$ and $\mathbf{B}$) can be found in [18], [19] and [20]. In addition, this 2D FE model can be easily extended to 3D deformation by changing the triangle mesh to tetrahedral mesh and adding the z-axis components in all the matrices and vectors.

III. ESTIMATION OF PHYSICAL PROPERTY

The FE dynamic model presented in last Section can be employed to simulate sweets-like objects. However, before simulating any real objects, important physical parameters must be available. In our FE model, there are totally 6 physical parameters: two elastic modulus E_1 and E_2, three viscous modulus c_1, c_2, and c_3, and Poisson's ratio γ. For parameter identification, the most popular and efficient method is optimization; *i.e.*, the simulation is iterated with updated physical parameters until the difference between the simulation and experiment becomes minimal. Therefore in this paper, we employed this optimization method to identify the physical parameters for our FE model.

In our previous work [20], we found that the Poisson's ratio γ can be estimated separately by minimizing the differences of keep-shape (the shape when the object was maintained before releasing). In [22], we found that there is a contradiction phenomenon between final-shape optimization and force optimization. It is impossible to reproduce both final-shape and force approximation simultaneously by using only one set of parameters due to the linearity of physical model.

In this paper, we therefore propose an identification method with two sets of parameters. Each set of them takes the responsibility to cover force response and final-shape, respectively. This method can be summarized as three steps. In the first step, we separately identify the Poisson's ratio γ by optimizing the keep-shape. In the second step, we use all the other 5 parameters as unknown variables to optimize force differences between simulation and experiment, as shown in Fig. 3a. We could obtain good force approximations using this set of parameters. In the third step, we only use parameter c_3 as unknown to optimize the difference of final-shapes, as shown in Fig. 3b, because parameter c_3 dominates the final-shape. The other parameters during the third step keep constants with the same values as identified in the second step. By using the second set of parameters (actually only parameter c_3 is different with the first set), we could reach a good approximation of final-shape.

The next issue is how to use these two sets of parameters to simulate an object under arbitrary operations. The first idea is to switch one set to another at some particular moment during simulation. Since the second set of parameters only affect the final-shape and should take effect after releasing, we can switch from the first parameter set to the second at the moment when the operation start to remove. However, it is not a good idea to use time as a switch criterion since the removing time is unavailable in advance for an arbitrary operation. Actually, there is no perfect switch criterion for an arbitrary operation. For example, if an object is subjected to several different operations which are not synchronous, it is impossible simulate these behaviors by switching parameter sets. Therefore we have to use both sets of parameters through the entire simulation time.

As shown in Fig. 4, two sets of parameters $\mathbf{x}^\star_{force}$ and $\mathbf{x}^\star_{shape}$ were input into simulation. Inside the simulator, actually, two objects with same structure and boundary conditions were simulated using these two parameter sets. After simulation, both objects have their own results of force and shape. The object simulated with parameter set $\mathbf{x}^\star_{force}$ provides correct force results but wrong shape results, and

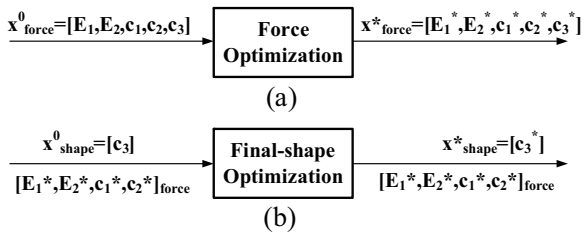

Fig. 3. Optimization processes for estimating two sets of parameters.

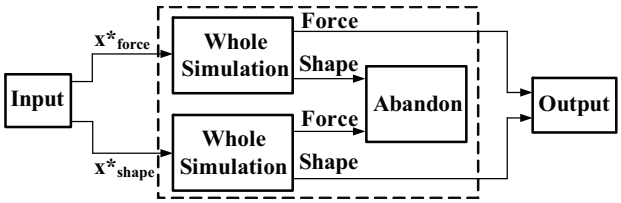

Fig. 4. Simulation process with two sets of parameters.

similarly the object simulated with $\mathbf{x}^{\star}_{shape}$ yields correct shape results but wrong force ones. After simulation, we therefore only output the correct results of shape and force from both simulations and discard the wrong ones. The process surrounded by the dash line in Fig. 4 worked like a black box since we only care about the input and output. This simulation procedure can yield good approximations for both deformed shapes and force behaviors. In next Section, we demonstrate some experimental results to validate our model and the parameter estimation approach.

IV. EXPERIMENT AND VALIDATION

A. Experimental Setup

The experimental materials were provided by OIMATU, a sweets company in Kyoto. Three kinds of materials with different properties were tested. They were made by flour, water, and bean powder mixed with a specific ratio. Three flat squared objects (each made by one material) were prepared for compression tests. Since the thickness of the objects is around 20% of the surface size, the deformation behaviors were treated as 2D case. The entire top surfaces of these objects were pushed down by a motorized stage with a constant velocity of 0.2 mm/s during time 0 to t_p. Before releasing, the deformed objects were maintained during time t_p to $(t_p + t_k)$. Some markers were drawn on the surfaces using a resist pen. The initial shapes, keep-shapes, and final-shapes were recorded by a camera, and the force data on the bottom surface were measured by a tactile sensor. Figures 5a, 5b, and 5c show the keep-shapes of these three objects. The shape and force data from these experimental trials were employed to identify the physical parameters for each material. In addition, three trials with 3-layered objects (each made by two kinds of materials) were performed to validate the identified parameters. The keep-shapes of these layered objects are shown in Fig. 5d, 5e, and 5f. Detailed information of these experiments is given in Table I.

B. Parameter Identification Results

Generally, the material property of an object will not differ even though it is subjected to different operations or it has different shape or size. This feature allows us to use regular-shaped objects with simple pushing operations to identify their physical parameters. Then, the identified parameters are able to simulate arbitrary-shaped objects with any operations. In our experiments, we used flat-squared objects pushed on the entire top surface with constant velocities. The parameter identification process can be divided into three steps as presented in Section 3. They are (1) estimation of Poisson's ratio

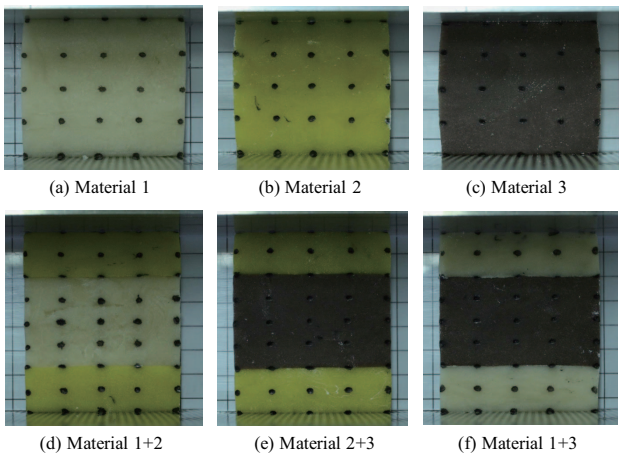

(a) Material 1 (b) Material 2 (c) Material 3

(d) Material 1+2 (e) Material 2+3 (f) Material 1+3

Fig. 5. The keep-shapes in different experimental trials.

TABLE I
DETAILED INFORMATION OF ALL EXPERIMENTAL TRIALS

Material	Object weight (g)	Object size W (mm)	H (mm)	T (mm)	Push velo. (mm/s)	Push disp. (mm)	Time t_p (s)	t_k (s)
Mat. 1	52.43	58.0	59.5	12.0	0.2	6	28.87	182.06
Mat. 2	32.97	50.0	50.0	11.0	0.2	6	29.68	181.26
Mat. 3	34.99	50.0	50.0	11.0	0.2	6	29.97	181.46
Mat. 1+2	66.99	60.0	80.0	11.0	0.2	10	49.29	181.76
Mat. 2+3	69.12	60.0	80.0	11.0	0.2	10	49.49	181.47
Mat. 1+3	68.52	60.0	80.0	11.0	0.2	10	49.49	181.97

γ by optimizing the keep-shapes; (2) identification of the first set of parameters by minimizing the force differences; and (3) identification of the second parameter c_3 by minimizing the differences of final-shapes while the other parameters are set to the values obtained from the first two steps. The objective functions for these three optimization problems can be uniformly formulated as

$$E(\theta) = \sum_{i=1}^{n} \|\mathbf{x}_i^{sim}(\theta) - \mathbf{x}_i^{exp}\|^2, \tag{9}$$

where $\mathbf{x}_i^{sim}$ and $\mathbf{x}_i^{exp}$ denote the data from simulation and experiment, respectively. In shape optimizations (the first and third steps), these two vectors are displacements of nodal points. In force optimization (the second step), they are force data on each sampling time. Vector θ denotes the parameters to be identified. They are $\theta = [\gamma]$, $\theta = [E_1, E_2, c_1, c_2, c3]^{\mathrm{T}}$, and $\theta = [c_3]$ in the first, second, and third steps, respectively. Three optimization problems were solved by the optimization toolbox of MATLAB with 'Nonlinear Least Squares' algorithm. The optimizations are terminated when the tolerance on objective function $E(\theta)$ or tolerance on vector θ is less than 1×10^{-6}.

For each material, we performed several optimization trials with different initial parameter values. The best solutions were chosen based on the objective function value $E(\theta)$. The final solutions of identified parameters are listed in Table

TABLE II

IDENTIFICATION RESULTS FOR THREE KINDS OF MATERIALS.

Mat. No.	Para. Sets	γ	E_1 (MPa)	E_2 (MPa)	c_1 (MPa·s)	c_2 (MPa·s)	c_3 (MPa·s)	$E(\theta)$
Mat1	$\mathbf{x}^\star_{force}$	0.3746	0.0349	0.0221	0.0071	0.1869	29.719	0.9038
	$\mathbf{x}^\star_{shape}$						1.4951	3.8141
Mat2	$\mathbf{x}^\star_{force}$	0.3353	0.0454	0.0141	0.0115	0.1991	13.370	1.3473
	$\mathbf{x}^\star_{shape}$						0.8987	2.4249
Mat3	$\mathbf{x}^\star_{force}$	0.3267	0.0575	0.0113	0.0172	0.1954	8.3936	0.6950
	$\mathbf{x}^\star_{shape}$						1.1421	3.2723

II. Note that only parameter c_3 is different between two sets of parameters. In order to reach a good approximation of final-shape, smaller value of parameter c_3 is necessary, as shown in Table II. Next subsection presents simulation results compared with experimental results to validate the identified parameters.

C. Validation and Discussion

With the parameters listed in Table II, we are able to simulate the experimental trials shown in Fig. 5. By using the simulation process shown in Fig. 4, we first simulated the material 1. The simulation results compared with experimental ones are shown in Fig. 6. Here we gave both output results and abandoned results. Note that if we only use one set of parameters, such as $\mathbf{x}^\star_{force}$, the simulation results would be Figs. 6a-1, 6b-2, and 6b-3. On the contrary, the parameter set $\mathbf{x}^\star_{shape}$ yielded Figs. 6b-1, 6a-2, and 6a-3. This indicated a contradiction between force and final-shape approximation and one set of parameters could not reproduce both force and final-shape simultaneously. This phenomenon comes from the linearity of five-element physical model and it can not be avoided by adding more elements [22]. This is the reason of using two sets of parameters to reach good approximation for both force and final-shape. From Figs. 6a-2 and 6b-2, we found that different parameter sets did not affect the keep-shapes, which again proved Poisson's ratio

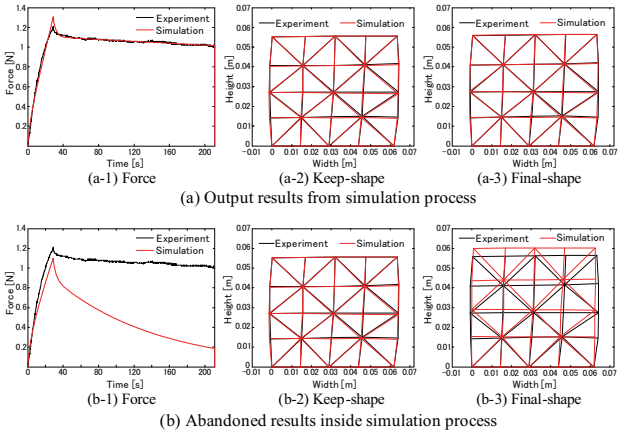

(a-1) Force (a-2) Keep-shape (a-3) Final-shape

(a) Output results from simulation process

(b-1) Force (b-2) Keep-shape (b-3) Final-shape

(b) Abandoned results inside simulation process

Fig. 6. Simulation results of material 1 compared with experiment data.

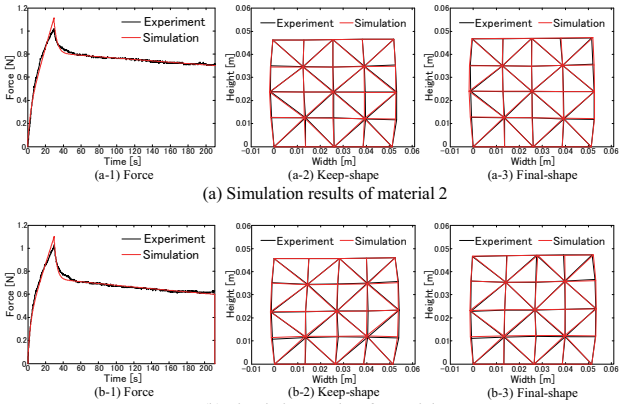

(a-1) Force (a-2) Keep-shape (a-3) Final-shape

(a) Simulation results of material 2

(b-1) Force (b-2) Keep-shape (b-3) Final-shape

(b) Simulation results of material 3

Fig. 7. Simulation results of material 2 and 3.

dominating the keep-shape. Simulations of material 2 and 3 were also performed and output results were shown in Fig. 7. We successfully reproduced both deformed shapes and force behaviors simultaneously by using two set of parameters.

Simulation results shown in Fig. 6 and Fig. 7 were simulated with their own optimized parameters. In other words, these simulation results just showed how good the optimizations were performed. It is quite insufficient. We therefore introduced three other experimental trials with layered objects, as shown in Figs. 5d, 5e, and 5f, to further validate the identified parameters. Each object consists of three layers with two different materials. Materials of the top layer and bottom layer were the same. This structure may be often encountered when dealing with sweets products. Different combinations of two materials were tested. The objects were pushed on the entire top surfaces with constant velocity of 0.2 mm/s. Detailed experimental information can be found in Table I. Estimated parameters listed in Table II were then used to simulate the deformation behaviors of these layered objects. The simulation results compared with experimental ones were shown in Fig. 8. We successfully reproduced both deformed shapes and force behaviors for these layered objects.

V. CONCLUSION AND FUTURE WORK

In this paper, the five-element physical model was introduced to describe the rheological behaviors of sweets-like objects. Comparing with three-element and four-element models, it provided more accurate results without any vibration. By imposing a five-element model on each triangle, 2D FE dynamic model was formulated for simulating the manufactural process of Japanese sweets. Based on this FE model, we proposed a method for estimating the physical parameters. In order to reproduce the deformed shapes and force behaviors simultaneously, this identification method involved three optimization steps: (1) the keep-shape optimization, (2) the force optimization, and (3) the final-shape optimization. Two sets of parameters were estimated and used to simulate rheological behaviors of the objects. Our FE model and parameter estimation method were applied

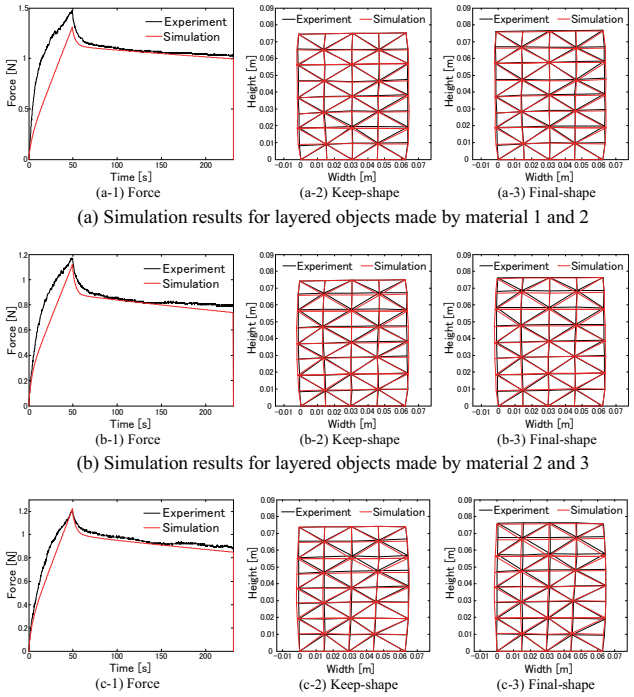

(a-1) Force (a-2) Keep-shape (a-3) Final-shape

(a) Simulation results for layered objects made by material 1 and 2

(b-1) Force (b-2) Keep-shape (b-3) Final-shape

(b) Simulation results for layered objects made by material 2 and 3

(c-1) Force (c-2) Keep-shape (c-3) Final-shape

(c) Simulation results for layered objects made by material 3 and 1

Fig. 8. Simulation results of three-layered objects compared with experiment data.

to three kinds of materials provided by a Japanese sweets company. The validation results showed that we successfully reproduced both deformed shapes and force behaviors simultaneously for uniform and layered objects. This FE model and identification method are suitable for simulating any sweets-like objects under any operations.

In the future, nonlinear physical models should be introduced into our FE model to develop more accurate model for simulating such sweets-like objects. Experiments with irregular-shaped and 3-dimensional objects will be performed to validate FE model and parameter estimation method. In addition, contact model between objects and human finger or tools will be investigated to simulate manufacturing process of sweets.

VI. ACKNOWLEDGMENTS

This research is supported in part by Grant in Aid for Scientific Research (No. 17206024) and R-GIRO program of Ritsumeikan University.

REFERENCES

[1] D. Terzopoulos, J. Platt, A. Barr, and K. Fleischer, "Elastically Deformable Models," *Proc. 14th Annual Conference on Computer Graphics and Interactive Techniques (SIGGRAPH '87)*, Anaheim, 1987, pp. 205-214.

[2] D. Terzopoulos and K. Fleischer, "Modeling Inelatic Deformation: Viscoelasticity, Plasticity, Fracture," *Proc. 15th Annual Conference on Computer Graphics and Interactive Techniques (SIGGRAPH '88)*, Atlanta, 1988, pp. 269-278.

[3] S. Cotin, H. Delingette, and N. Ayache, Real-Time Elastic Deformations of Soft Tissues for Surgery Simulation, *IEEE Trans. Visualization and Computer Graphics*, vol. 5, no. 1, 1999, pp. 62-73.

[4] T. Inoue and S. Hirai, Elastic Model of Deformable Fingertip for Soft-Fingered Manipulation, *IEEE Trans. Robotics*, vol.22, no.6, 2006, pp. 1273-1279.

[5] S. Tokumoto, Y. Fujita, and S. Hirai, "Deformation Modeling of Viscoelastic Objects for Their Shape Control," *Proc. IEEE International Conference on Robotics and Automation (ICRA '99)*, vol. 1, 1999, pp. 767-772.

[6] A. Hamada, T. Tanaka, M. Kume, Y. Yoshida, A. Nakai, and T. Yoshida, "Finger Motion of Wrapping Process During Kyogashi Making," *17th World Congress on Ergonomics*, Beijing, 2009, pp. 283-287.

[7] K. Waters, "A Muscle Model for Animating Three-Dimensional Facial Expression," *Proc. 14th Annual Conference on Computer Graphics and Interactive Techniques (SIGGRAPH '87)*, Anaheim, 1987, pp. 17-24.

[8] D. L. James and D. K. Pai, "ArtDefo: Accurate Real Time Deformable Objects," *Proc. 26th Annual Conference on Computer Graphics and Interactive Techniques (SIGGRAPH '99)*, Los Angeles, 1999, pp. 65-72.

[9] M. B. Nielsen, S. Cotin, "Real-time Volumetric Deformable Models for Surgery Simulation Using Finite Elements and Condensation", *Computer Graphics Forum (Eurographics'96)*, Poitiers, 1996, pp. 57-66.

[10] H. Yoshida, Y. Murata, and H. Noborio, "A Smart Rheologic MSD Model Pushed/Calibrated/Evaluated by Experimental Impulses," *Proc. IEEE/RSJ International Conference on Intelligent Robots and Systems (IROS '05)*, Edmonton, 2005, pp. 269-276.

[11] T. Ikawa and H. Noborio, "On the Precision and Efficiency of Hierarchical Rheology MSD Model," *Proc. IEEE/RSJ International Conference on Intelligent Robots and Systems (IROS '07)*, San Diego, 2007, pp. 376-383.

[12] N. Sakamoto, M. Higashimori, T. Tsuji, and M. Kaneko, "An Optimum Design of Robotic Hand for Handling a Visco-elastic Object Based on Maxwell Model," *Proc. IEEE International Conference on Robotics and Automation (ICRA '07)*, Roma, 2007, pp. 1219-1225.

[13] C.-H.D. Tsai, I. Kao, N. Sakamoto, M. Higashimori, and M. Kaneko, "Applying Viscoelastic Contact Modeling to Grasping Task: An Experimental Case Study," *Proc. IEEE/RSJ International Conference on Intelligent Robots and Systems (IROS '08)*, Nice, 2008, pp. 1790-1795.

[14] Y.-H. Chai, G. R. Luecke, and J. C. Edwards, "Virtual Clay Modeling Using the ISU Exoskeleton," *Proc. IEEE Virtual Reality Annual International Symposium (VRAIS '98)*, Atlanta, 1998, pp. 76-80.

[15] M. Kimura, Y. Sugiyama, S. Tomokuni, and S. Hirai, "Constructing Rheologically Deformable Virtual Objects," *Proc. IEEE International Conference on Robotics and Automation (ICRA '03)*, Taipei, 2003, pp. 3737-3743.

[16] S. Tokumoto, Y. Fujita, and S. Hirai, "Deformation Modeling of Viscoelastic Objects for Their Shape Control," *Proc. IEEE International Conference on Robotics and Automation (ICRA '99)*, Detroit, 1999, pp. 767-772.

[17] N. Ueda, S. Hirai, and H. T. Tanaka, "Extracting Rheological Properties of Deformable Objects with Haptic Vision," *Proc. IEEE International Conference on Robotics and Automation (ICRA '04)*, Barcelona, 2004, pp. 3902-3907.

[18] J. Muramatsu, T. Ikuta, S. Hirai, and S. Morikawa, "Validation of FE Deformation Models using Ultrasonic and MR Images," *The 9th International Conference on Control, Automation, Robotics and Vision (ICARCV '06)*, Singapore, 2006, pp. 1-6.

[19] Z. Wang, K. Namima, and S. Hirai, "Physical Parameter Identification of Rheological Object Based on Measurement of Deformation and Force," *Proc. IEEE International Conference on Robotics and Automation (ICRA '09)*, Kobe, 2009, pp. 1238-1243.

[20] Z. Wang and S. Hirai, "Modeling and Parameter Identification of Rheological Object Based on FE Method and Nonlinear Optimization," *Proc. IEEE/RSJ International Conference on Intelligent Robots and Systems (IROS '09)*, St. Louis, 2009, pp. 1968-1973.

[21] J. Baumgarte, "Stabilization of Constraints and Integrals of Motion in Dynamical Systems," *Computer Methods in Applied Mechanics and Engineering*, vol.1, no.1, 1972, pp. 1-16.

[22] Z. Wang and S. Hirai, "Modeling and Parameter Estimation of Rheological Objects for Simultaneous Reproduction of Force and Deformation," Submitted to *the 1st International Conference on Applied Bionics and Biomechanics*, Venice, 2010.